COHERENT RADIATION STUDIES FOR THE FERMI@ELETTRA RELATIVE BUNCH LENGTH DIAGNOSTICS

S. Di Mitri, M. Ferianis, M. Veronese*, Sincrotrone Trieste, Trieste, Italy

Abstract

Bunch compressors are key components of the seeded FEL FERMI@Elettra. Assuring their stable operation requires multiple non-destructive diagnostics to provide error signals to the feedback systems. Both the energy and the peak current of the electron bunch have to be stabilized by the feedback systems. The peak current stabilization implies charge and bunch length stabilization. The latter will be achieved by a redundant diagnostics based on Coherent Synchrotron Radiation (CSR) and Coherent Diffraction Radiation (CDR). In this paper we describe a study of Coherent Radiation emission downstream bunch compressors as the source of a relative bunch length measurement. The study evaluates the most critical parameters in the design of such a diagnostic using numerical integration to calculate the spectral angular properties of the radiation for both CSR and CDR.

COHERENT RADIATION EMISSION.

An introduction to the main concepts related to the coherent radiation emission can be found in ref.[1]. The spectral angular intensity distribution of a N-electrons bunch is related to the spectral angular distribution of a single electron as shown in eq.1.

$$\frac{d^2I}{d\nu d\Omega} = \left[N + N\left(N-1\right)\left|F(\rho)\right|^2\right] \frac{d^2I}{d\nu d\Omega}_{1e-} \qquad (1)$$

Where $F(\rho)$ is the Fourier transform of the longitudinal normalized bunch distribution $\rho(t)$. The total N-electron spectral angular distribution is the sum of the incoherent term ($\propto N$) and a coherent term ($\propto N^2$). The frequency behavior of the coherent contribution depends on the square of the Fourier Transform of $\rho(t)$. As the bunch gets shorter, the F($\rho(t)$) becomes spectrally broader and the emitted power increases. To evaluate the emission properties (spectral distribution and intensity) we have computed the coherent spectral angular distribution in two steps. In the first we have calculated F($\rho(t)$), by means of the FFT of the bunch profile derived from Elegant simulations at the exit of the bunch compressors (or by a rectangular approximation of it). In the second we have used a numerical code to calculate the single electron spectral-angular distribution. This approach has been used for CSR and CDR.

* marco.veronese@elettra.trieste.it

Table 1: Parameters used in the calculation.

Parameter	BC1	BC2
Energy [MeV]	220	600
Dipole length [m]	0.5	0.5
Dipole field [T]	0.1(M, L)	0.2(M) 0.32(L)
Dipoles distance [m]	2.5	2.5
Detector size [mm]	30x30	30x30
Charge [nC]	0.8(M) 1(L)	0.8(M) 1(L)
Bunch length [ps]	2.8(M) 5.4(L)	0.7(M) 1.8(L)

COHERENT SYNCHROTRON RADIATION

The calculation of the 1-electron spectral angular distribution of synchrotron radiation has been performed using a Matlab code written by O.Grimm (DESY) which performs a single electron tracking through an arbitrary magnetic field. The code is based on the Liénard Wiechert potentials:

$$\vec{E} = \frac{e}{4\pi\epsilon_0}\left\{\frac{(\vec{n}-\vec{\beta})}{\gamma^2(1-\vec{n}\vec{\beta})^3R^2} + \frac{\vec{n}\times((\vec{n}-\vec{\beta})\times\vec{\beta})}{c(1-\vec{n}\vec{\beta})^3R}\right\} \qquad (2)$$

Where $\vec{n}$ is the vector from the initial position to the observation point, R is the distance between the initial position and the observation point, while $\vec{\beta}$ is the vector velocity divided by c (the speed of light) and $\vec{\beta'} = d\vec{\beta}/dt$ is the acceleration, finally γ is the Lorentz factor. The first term of eq. 2 is known as velocity term and the second as acceleration term. In our case both terms have to be considered together with the finite size of the magnets (see [2]).

The spectral angular distribution is calculated as the sum of the different contribution of the Fourier transforms of the electric field along the particle trajectory:

$$\frac{d^2I}{d\nu d\Omega}_{1el.} = 2\epsilon_0 c\left[\left|F_x^2\right| + \left|F_y^2\right| + \left|F_z^2\right|\right] \qquad (3)$$

Where the F_k are the sums over j (the particle tracking step) of the phase components:

$$F_k = \sum_j \frac{1}{2\pi i} E_{j-1}(\vec{r}_{ret}) e^{-2\pi i\nu t_{j-1}}(1 - e^{-2\pi i\nu\Delta t}) \quad (4)$$

The parameters used in the simulation are listed in Table 1, where (M) and (L) mean respectively $Medium$ and $Long$ bunches. In the simulation we have considered not only the emission from the fourth dipole of the chicane but also from the third dipole and accounted for the shielding (low frequency cut-off) due to the vacuum chambers walls using the mirror charges approach (see e.g. [3]) for perfectly conducting planes.

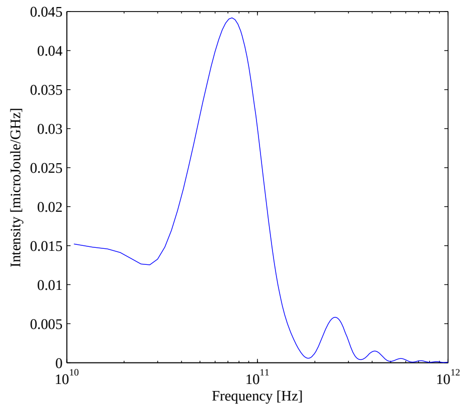

Figure 1: CSR spectral distribution for BC1 *Medium Bunch*.

Fig.1 shows the spectral distribution obtained for BC1 *Long Bunch* integrating over the detector. The detector corresponds to an area of 30x30mm whose origin is centered transversally 25mm away from the electron beam trajectory and is placed 150mm downstream the exit of the 4^{th} dipole of BC1. The intensity distribution at the detector is shown in Fig. 2.

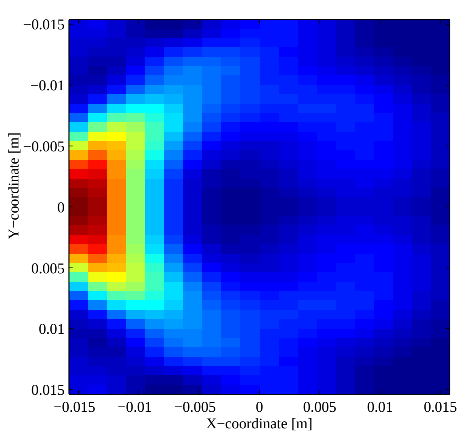

Figure 2: BC1 *long bunch* intensity distribution at the detector.

The calculated values of energy per pulse for BC1 and BC2 in the *Medium* and *Long* cases are summarized in Table 2. The first frequency range is the one of the calculation, the second accounts for the limited pyroelectric detectors spectral sensitivity. The emitted energy increases the shorter are the bunches. For BC2 we can expect a higher CSR intensity than for BC1.
Other approaches to the problem are possible as done in [4]

Table 2: CSR emitted energy per bunch.

Range	**BC1-M**	**BC1-L**	**BC2-M**	**BC2-L**
0.01-1 THz	11 μJ	4.1 μJ	66 μJ	27 μJ
0.15-1 THz	1.5 μJ	0.3 μJ	46 μJ	8 μJ

for the BC1 of LCSL where the CSR has been studied via an integral formulation.

COHERENT DIFFRACTION RADIATION

To calculate the spectral angular distribution of CDR in near field we have used a numerical approach to the analytical treatment described in [5] (see also [6]).
For FERMI *Medium bunch*, and *Long bunch*, both the large target size approximation ($a >> \gamma\lambda$) and the far field approximation ($D >> \gamma^2\lambda$) are violated. Here a is the radius of the emitter screen, D is the distance between the detector and the screen planes, λ is the wavelength of the emitted radiation and γ is the Lorentz factor. As an example we can take BC1 *long* bunch ($\lambda = 3mm$ and $\gamma = 430$) then the first condition is satisfied for $a > 1.3m$ and the second for $D > 600m$. The diffraction radiation emission spectral angular distribution has be calculated evaluating numerically:

$$\frac{d^2I}{d\nu d\Omega} = \frac{4e^2k^4}{(2\pi)^2\epsilon_0\beta^4\gamma^2c} \times \left| \int_b^a K_1\left(\frac{k\rho}{\beta\gamma}\right) e^{\left(\frac{ik\rho^2}{2D/cos\theta}\right)} J_1(k\rho sin\theta)\rho d\rho \right|^2 \quad (5)$$

This expression is the diffraction radiation equivalent of expression for transition radiation in ref. [5]. Here b is the hole radius, ρ is the distance from the screen center to a point on the screen in cylindrical coordinate and θ is the angle between the center of the screen and the point of observation P on the detector plane. Equation 5 gives, in the limit of $b \to 0$, the transition radiation expression in near field, moreover in the limits of $a, D \to \infty$ it gives to the Ginzburg-Frank formula.
We have first investigated the effect of near field. Fig. 4 shows the Coherent Transition Radiation (CTR) spectrum at BC2 for the *medium bunch* as a function of the distance D between the plane of the transition radiation screen and the plane of observation. The change from the far-field regime to the near field regime is shown as a suppression of intensity as the distance D decreases. Even though the far field condition in this case would state $D >> 3947$ m at 100 GHz, the expected intensity suppression in near field, becomes noticeable approximately for $D < 1$ m.

From all figures is is clear there is a relevant benefit in using the largest possible angular acceptance and screen radius. The screen radius used in the calculation is 60mm and the

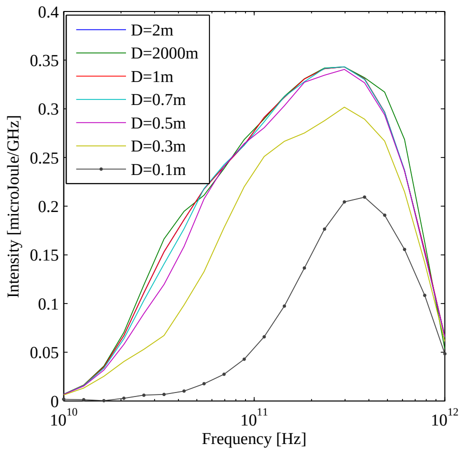

Figure 3: CTR for BC2 *Medium Bunch* as a function of distance D with angular acceptance of 0.1rad and 0.2rad

angular acceptance is 0.1 rad (0.2 rad calculation are plotted for comparison).

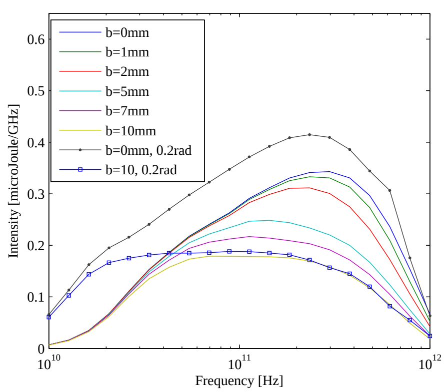

Figure 4: CDR for BC2 *Medium Bunch* as a function of the hole radius b of angular acceptance of 0.1rad and 0.2rad

The choice of the hole radius for a CDR emitter is important and should be done as a compromise between CDR intensity output and beam dynamics requirements in terms of wakefields induced by the screen. A hole radius of the order of 5-10 mm should radiate with sufficient intensity without giving major contributions to the wakefields budgets since the iris of the RF accelerating structures of FERMI are of the same order of magnitude and the total number of irises is about one thousand.

In particular for BC1 *Long bunch* (see Fig. 5) the hole radius b does not impact too much the integrated intensity for 0.1rad of angular acceptance in the range from 0 to 10mm, moreover when increasing to 0.2rad the angular acceptance of the system, we immediately gain spectral intensity below 70 GHz. The situation is different for BC2 *Medium* in Fig. 4 where the effect of the hole radius size is more pronounced while the use of larger angular acceptance is less important than in the case of BC1 *Long*. The CDR emitted intensity in terms of energy/bunch obtained by integration of the espctral distribution are reported in Table 3.

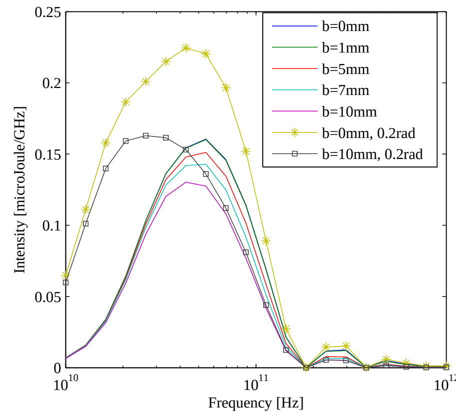

Figure 5: CDR for BC1 *Long Bunch* as a function of hole radius b of angular acceptance of 0.1rad and 0.2rad.

Table 3: CDR emitted energy per bunch, a=60mm, D=1m.

Bunch	**b=0mm 0.1rad**	**b=5mm 0.1rad**	**b=10mm 0.1rad**	**b=10mm 0.2rad**
BC1-L	17 μJ	14 μJ	11 μJ	14 μJ
BC2-M	233 μJ	146 μJ	105 μJ	110 μJ

CONCLUSIONS

We have studied the properties of both CSR and CDR radiation sources for the application to the relative bunch length measurement system of FERMI@Elettra. Both sources are capable to provide μJoule level energy pulses and are suitable for the foreseen application. A detailed knowledge of the influence of the main parameters on the coherent radiation emission is important to guarantee the needed performances of this diagnostics.

ACKNOWLEDGMENT

The authors would like to thank O. Grimm for providing his Matlab code and E. Chiadroni for useful discussions.

REFERENCES

[1] O. Grimm, pg.1040, Proc. FEL Conf. 2006 (2006)

[2] E.L. Saldin $et al.$, NIM-A, pg 373, v. 398 (1997)

[3] M. Dholus and T. Limberg, NIM-A, pg 278, v. 407 (1998)

[4] G. Stupakov $et al.$ pg.728, Proc. FEL Conf. 2006 (2006)

[5] S. Casalbuoni $et al.$ TESLA Report 2005-15 (2005)

[6] M.Castellano $et al.$, NIM-A pg. 297, v. 435 (1999)